THE EFFECT OF DIFFUSED HYDROGEN ON THE TORSIONAL FATIGUE LIFE OF 2024-T351 ALUMINUM ALLOY

by

Charles Joseph Kauffmann, Jr.

Thesis submitted to the Graduate Faculty of
Virginia Polytechnic Institute and State University
in partial fulfillment of the requirements for the degree of

MASTER OF SCIENCE

in

Mechanical Engineering

APPROVED:

H. H. Mabie, Chairman

N. S. Eiss, Jr.

L. D. Mitchell

March, 1978

Blacksburg, Virginia

ACKNOWLEDGMENTS

The author wishes to extend his sincere appreciation to his major professor, Dr. H. H. Mabie, for his cooperation and assistance provided throughout this investigation. A word of thanks is also extended to Dr. N. S. Eiss, Jr., and Dr. L. D. Mitchell for their help as members of the advisory committee.

Special gratitude is extended to of the Materials Engineering Department for the suggestion of this topic and to and of the Engineering Science and Mechanics Department for their advice and assistance during this investigation.

Finally, the author wishes to thank his wife for her help, patience, and encouragement.

TABLE OF CONTENTS

	Page
Acknowledgments	ii
List of Figures	iv
List of Tables	vi
Introduction	1
Literature Review	3
Experimental Objective	14
Test Apparatus	
Diffusion Equipment	15
Fatigue Equipment	15
Test Specimens	24
Test Procedure	29
Results	32
Discussion of Results	48
Conclusions	51
Recommendations	52
References	53
Appendices	
Appendix A. Statistical Analysis of Results	56
Appendix B. Test Equipment	62
Vita	64

LIST OF FIGURES

		Page
FIGURE 1.	Diffusion Equipment	16
FIGURE 2.	Schematic Drawing of Sonntag Universal Fatigue Testing Machine Components	17
FIGURE 3.	Sonntag Universal Fatigue Testing Machine With Environmental Chamber in Place	18
FIGURE 4.	Schematic Drawing of Torsional Fixture Components	19
FIGURE 5.	Torsional Fixture of Fatigue Testing Machine With Environmental Chamber in Place	21
FIGURE 6.	Schematic Drawing of Humidifying Equipment	22
FIGURE 7.	Test Specimen Dimensions	28
FIGURE 8.	Tests at High Relative Humidity for Charged Specimens	34
FIGURE 9.	Tests at High Relative Humidity for Uncharged Specimens	39
FIGURE 10.	Comparison of Tests at High Relative Humidity for Charged and Uncharged Specimens	40
FIGURE 11.	Tests at Low Relative Humidity for Charged Specimens	41
FIGURE 12.	Tests at Low Relative Humidity for Uncharged Specimens	42
FIGURE 13.	Comparison of Tests at Low Relative Humidity For Charged and Uncharged Specimens	43
FIGURE 14a.	Typical Crack Propagation in a Hydrogen-Charged Specimen at High Humidity.	44
FIGURE 14b.	Typical Crack Propagation in Uncharged Specimens and Low Humidity Charged Specimens	44
FIGURE 15.	Fracture Surface of a Hydrogen-Charged Specimen Showing Striations	45

LIST OF FIGURES (Cont'd)

		Page
FIGURE 16.	Fracture Surface of a Hydrogen-Charged Specimen Showing no Striations	46
FIGURE 17.	Fracture Surface of an Uncharged Specimen Showing no Striations	47

LIST OF TABLES

		Page
TABLE 1.	Typical Mechanical Properties of 2024-T351 Aluminum	25
TABLE 2.	Mechanical Property Limits of Extruded Shapes of 2024-T351 Aluminum	26
TABLE 3.	Chemical Composition of 2024 Aluminum	27
TABLE 4.	Results for Fatigue Tests	34
TABLE 5.	Results of Significance Tests	49
TABLE A-1.	Equations for S-N Diagrams	57
TABLE A-2.	Computations for Significance Tests	60

INTRODUCTION

Fatigue is a very complex phenomena which is dependent upon environmental conditions, microscopic and macroscopic conditions of the material, and the cyclic stressing the material undergoes. In corrosion fatigue, the repeated stressing and corrosive environment interact to cause accelerated failure of the material. This failure is usually sudden and unpredictable. Much of the research in corrosion fatigue has been on steels and aluminum.

Aluminum is used extensively in the aerospace field because of its low density and high strength. In such an application, it is important to know when corrosion fatigue can occur. It has been well documented that water vapor has a detrimental effect on aluminum and aluminum alloys under cyclic loads. However, the mechanism causing this phenomena is not understood. There are three basic theories proposed to explain this mechanism:

1. Hydrogen Theory - Hydrogen ions assist crack initiation and growth by: a) diffusing into voids causing a buildup of internal pressure, b) enhancing void formation, or c) lowering the surface energy.
2. Adsorption Theory - Formation of an oxide film on the crack surface prevents cyclic reversibility.
3. Oxide Film Property Theory - The properties of the oxide film are affected by the humidity. The oxide film affects the crack initiation and growth.

The objective of this investigation was to examine the hydrogen theory. This was done by studying the effect of diffused hydrogen on the torsional fatigue life of 2024-T351 aluminum at two humidity levels and three stress levels.

LITERATURE REVIEW

The possible detrimental effect of the environment on the fatigue life of metals had been revealed back in the early 1900's. Wadsworth (1,2)* in 1958 conducted fatigue tests on polycrystalline copper, pure aluminum, and gold at various pressures of air and other gases. He reported that water vapor reduced the fatigue life of aluminum by increasing the rate of crack propagation. In all cases, the first crack formed very early in the life of the specimen. Therefore, it was concluded that the surrounding atmosphere had no effect on crack initiation, only crack propagation. He theorized that the mechanism for crack propagation was chemical attack. The corrosive substance had to be present as a gas while fatiguing was in progress. The chemical attack occurred at the crack tip where the gas could assist crack growth in two ways. First, the gas could attack the highly strained metal, weaken it, and help to break it. Second, the gas could form an adsorbed film on the freshly exposed surfaces as they separate during the tension half cycle preventing the sides of the crack from sticking together again on the compressive half cycle.

Broom and Nicholson (3) in 1961 reported the results of their tests on three types of age-hardened aluminum alloys fatigued in air, in vacuum, and in other gaseous environments. The types of alloys were aluminum-4% copper alloy, L65 and D.T.D. 683 aluminum alloys.

---

*Numbers in parentheses refer to references listed at the end of this thesis.

In addition to water vapor, they determined that hydrogen gas had a significant effect on both crack initiation and crack growth in aluminum alloys. However, the effect of the hydrogen gas was appreciably smaller than that caused by water vapor. From this they concluded that hydrogen ions were responsible for reduced fatigue life and that these ions were released by the reaction of water vapor with aluminum or by dissociation of hydrogen molecules. They proposed that the introduction of hydrogen ions diffusing rapidly from the surface into the interior of the metal assisted crack initiation and accelerated crack growth in one of three ways:

1. Hydrogen ions diffuse into voids in the internal surface of the metal where they recombine with a low probability of dissociation. This leads to a buildup of internal presure in the voids.
2. Hydrogen ions associate with vacancies which enhances the chances of the vacancies clustering to form voids.
3. Hydrogen ions embrittle the aluminum by lowering the surface energy.

In 1962, Holshouser and Bennett (4) found that gas bubbles containing hydrogen formed under transparent pressure sensitive tape on the surface of aluminum alloy specimens in either torsional or bending fatigue. The gas bubbles which started to appear before cracks could be detected in the specimen indicated that hydrogen gas was produced during the crack initiation stage. After the crack was observed, the rate of gas evolution increased. They theorized that the bubbles

were formed by the reaction of absorbed water with freshly exposed metal. During the crack initiation period, the metal was exposed by cracking of the surface oxide film due to localized strain. During the crack propagation period, the cracks extended rapidly due to the large amount of fresh metal that was exposed from the wear that occurred as the walls of the crack rubbed together during the cylic stressing.

Laird and Smith (5) in 1963 studied the early stages of fatigue crack growth of pure aluminum, copper, and nickel in vacuum and in other atmospheres. They agreed with Wadsworth (1,2) that the effect of air on the fatigue of aluminum was to enhance crack growth by chemical attack at the crack root and that air had no effect on crack initiation. They also reported that the effect of the atmosphere decreased as the crack depth increased. They regarded this as evidence supporting the chemical-attack mechanism vs. the self-healing or welding mechanism to explain fatigue crack growth inhibition in inert atmospheres.

Bennett (6) in 1963 reported that water vapor was the only atmospheric component that affected the fatigue life of many aluminum alloys. In experiments with aluminum alloys where the humidity was changed during the tests, he found that during crack initiation the humidity had no effect on the fatigue life, but during the crack propagation period there was a very marked effect. He suggested that during crack initiation the deformations were uniformly distributed so that the oxide film remained intact and no reactions occurred. As the

stressing continued, the deformations became localized causing the oxide film to rupture in severely strained regions exposing fresh metal. The fresh metal was rapidly oxidized so that reverse slip could not occur on the same plane. Therefore, the damage caused by cyclic slipping accumulated. He realized, however, that this explanation could not account for the fact that oxygen had no effect on the life of aluminum alloys.

In 1965, Hartman (7) found that oxygen in the air also increased the crack propagation rate of 2024-T3 Alclad sheet at low stress amplitude or short crack length, but the effect of water vapor on fatigue crack growth predominated over that of oxygen. Because of the affinity of the aluminum oxide layer to adsorb water molecules, he proposed that the amount of water vapor in the air was not as important as the amount of water adsorbed by the oxide layer. When plastic deformations of the metal initiated cracks in the oxide layer, two events took place. First, water molecules entered the crack and reacted with the fresh aluminum surface forming an oxide film. This film prevented the complete reversibility of the movement which produced the crack and thus promoted crack growth. Second, the reaction of the water molecules with aluminum ions formed hydrogen ions ($Al + 3H_2O = Al_2O_3 + 6H^+ + 6e^-$). These hydrogen ions diffused into the metal and at voids picked up electrons from the metal becoming hydrogen atoms. The localized hydrogen gas produced large internal stresses which were superimposed on the applied external stresses accelerating the crack growth rate. Hartman concluded that the second mechanism was the more influential of the two.

Hordon (8) in 1966 agreed with Hartman (7) that both oxygen adsorption on the freshly formed crack surfaces forming aluminum oxide and the adsorption of hydrogen ions through crack surfaces were both likely to operate during the crack growth phase of the fatigue process. He went on to show through kinetic relationships and experiments that adsorption rates at pressures below 1×10^{-3} torr [0.1 Pa] were too slow to enhance crack growth rates. As a result of his work, Hordon concluded that oxygen adsorption into the fatigue crack was the critical mechanism.

In 1966, Bradshaw and Wheeler (9) reported their work on the effect of the environment on fatigue crack growth in three types of aluminum: 1) a clad aluminum-copper-magnesium alloy, DTD 5070A, 2) a 99.99 percent pure, cold-worked aluminum, and 3) a sintered aluminum powder, SAP 895. They found that oxygen had an effect at low crack rates only. This was attributed to oxides forming which blocked reverse slip. However, water vapor was the dominant component in the environment which affected crack growth rates at pressures above ~0.5 torr [67 Pa]. This was the pressure above which the water vapor could overcome the impedance of the crack and reach the crack tip. They concluded that Broom's hydrogen theory fit their observations best.

Eeles and Thurston (10) in 1967 studied the effect of humidity on the oxide film of Alclad 575 aluminum alloy. They postulated that changes in the fatigue lives at different humidities were primarily caused by differences in the oxide films formed in the environments

of different humidities. They also suggested that a crack in the oxide film could cause a strain in the base metal such that a dislocation would be generated from which a crack could initiate.

Grosskreutz (11) in 1967 fatigued aluminum single crystals in air and in vacuum. He found that the Young's modulus for the aluminum oxide film increased by a factor of four under vacuum vs. air. He postulated that this was due to the removal of adsorbed water vapor from the oxide film in vacuum. This theory tended to strengthen Eeles and Thurston's theory (10).

In 1968, Meyn (12,13) reported from experimental observation and data that two mechanisms of crack propagation existed for 2024 aluminum in fatigue. At low cyclic amplitudes--crack propagation rates of 0.3μ [0.3 x 10^{-6}m] per cycle or less--the cracks grew by tensile cracking caused by the combination of the crack-tip stress and the constituents in the air. At high amplitudes--crack propagation rates above 0.5μ [0.5 x 10^{-6}m] per cycle--the crack propagation mechanism became one of ductile tearing at the crack tip, followed by compressive resharpening of the crack tip.

Wright and Hordon (14) in 1968 studied the effect of oxygen, water vapor, and hydrogen on 1100-H14 aluminum at pressures from 1 x 10^{3} to 1 x 10^{-7} torr [1 x 10^{5} to 1 x 10^{-5} Pa] . A reduced fatigue life was observed at partial pressures greater than 1 x 10^{-3} torr [0.1 Pa] if either oxygen or water vapor was present. For hydrogen, the fatigue resistance typical of high-vacuum environments was retained up to a pressure of approximately 1 torr [1 x 10^{2} Pa].

Wei (15) in 1968 performed fatigue tests on 7075-T651 aluminum alloy at temperatures ranging from room temperature to 100°C in environments of hydrogen, oxygen, and distilled water. His results indicated that fatigue-crack propagation was controlled by a thermally activated process. The activation energy for this process was strongly dependent on the crack tip stress intensity factor (ΔK). The rate-controlling step for crack propagation in the range of crack growth rates of 1×10^{-6} to 1×10^{-5} inch [3×10^{-5} to 3×10^{-4}mm] per cycle was the creation of new crack surfaces. He interpreted his results as agreeing with the previously proposed theory that the cause for an increase in the crack propagation rate in a water vapor environment was the reaction of the water with freshly created aluminum crack surfaces forming hydrogen gas at high pressures which diffuses into the region ahead of the crack tip.

Engelmaier (16) in 1968 conducted fatigue tests on 2024-T3 aluminum alloy in vacuum and in air. He reported that intergranular cracking started before the first 10% of the fatigue life of the specimen and occurred until the last 5% of the fatigue life of the specimen, at which time transgranular cracking started. This transition stage was the stage reported most sensitive to the environment.

Achter (17) in 1968 proposed a kinetic model for calculating the critical pressure (pressure at which the rate of adsorption of a gas by the crack surface equals the rate of crack surface generation) which predicted a value of critical pressure for aluminum in water vapor close to the observed critical pressure. This result supported

the adsorption model (reactions at the surface prevent complete reversibility) for the effect of the environment on fatigue-crack propagation.

In 1969, Wei and Landes (18) investigated the effect of D_2O on fatigue crack propagation in 7075-T651 aluminum alloy. The results were essentially the same as Wei had found previously (15) using distilled water. They confirmed the conclusion that the rate-controlling process in fatigue-crack propagation of aluminum alloys was the mechanical process of creating new crack surfaces and was not the transport of the water to the crack tip or hydrogen ion diffusion into the material ahead of the crack tip.

Vennett and Ansell (19) in 1969 reported that there was no loss in properties or change in fracture behavior in 7039-T61 aluminum alloy tested in hydrogen environments up to 10,000 psi [68.95 MPa] .

McCarroll and Anderson (20) in 1969 reported that hydrogen atoms adsorbed on clean aluminum films at 77K [$-320^{\circ}F$] and that when warmed to room temperature not all of the hydrogen was recovered, indicating some solubility of hydrogen in the aluminum. However, hydrogen molecules did not react with the clean aluminum films at either 77K [$-320^{\circ}F$] or 300K [$81^{\circ}F$].

George (21) in 1971 studied the effect of relative humidity upon the ultrasonic fatigue endurance of L65 aluminum alloy. The tests were run at 20,000 Hz giving a fatigue life of minutes and a crack propagation period of only a few seconds. He concluded that hydrogen diffusion, especially during the crack propagation period,

was not likely to occur in such a short period of time. He concluded that the theory of variations in the mechanical properties of the oxide film with different environmental humidities and the oxide film fracture as a source of crack initiation to be a more acceptable theory than the adsorption or hydrogen theories.

Louthan, Caskey, Donovan and Rawl (22) in 1972 investigated the effect of hydrogen on different metals. For 7039 aluminum, they found essentially no change in tensile properties after exposure to 10,000 psi [68.95 MPa] hydrogen at 71°C [160°F] for 524 days compared to the properties in air. The hydrogen concentration in the aluminum after this exposure was reported as nil. For 2011 and 7039 aluminum alloys, there were essentially no changes again in tensile properties when tested in a 10,000 psi [68.95 MPa] hydrogen environment compared to the properties in a 10,000 psi [68.95 MPa] helium environment. For tritium-charged 5086 aluminum, the rate of tritium released during deformation increased as the amount of dislocation movement increased. They concluded that this demonstrated that hydrogen in hydrogen-charged specimens moves with dislocations.

In 1973, Jewett, Walter, Chandler and Frohmberg (23) reported on their study of hydrogen embrittlement of metals. They claimed that aluminum alloys could not be embrittled from internal hydrogen or from environmental hydrogen.

McLellan and Harkins (24) in 1975 reported that aluminum did not chemisorb hydrogen or form metallic hydrides and, therefore, was immune to low temperature hydrogen embrittlement. High temperature

attack was also said not to occur since the oxides of aluminum are irreducible by hydrogen.

As can be seen from the above review, no one is certain as to the reason for the effect of water vapor on the fatigue life of aluminum. The conclusions generally fall into three basic theories:

1. Hydrogen Theory - Hydrogen ions assist crack initiation and growth by diffusing into voids causing a buildup of internal pressure, by enhancing void formation, or by lowering the surface energy.
2. Adsorption Theory - Formation of an oxide film on the crack surface prevents cyclic reversibility.
3. Oxide Film Property Theory - The properties of the oxide film are affected by the humidity and the oxide film affects the crack initiation and growth.

The hydrogen theory is strengthened by recent literature in the field of stress corrosion cracking. Speidel (25) in 1973 concluded that stress-corrosion cracking of aluminum alloys in gaseous atmospheres containing water vapor was the result of hydrogen embrittlement. He theorized that the reason dry molecular and dry atomic hydrogen gas did not cause hydrogen embrittlement was that the fugacities were not high enough, but that the reaction of water with pure aluminum and the subsequent release of hydrogen ions at the crack tip caused a substantially higher fugacity for the hydrogen.

In 1974, Gest and Troiano (26) demonstrated hydrogen embrittlement for 7075-T651 aluminum alloy. After cathodically charging the

samples with hydrogen in a 3% NaCl solution, they observed a reversible ductility loss with strain-rate dependence and temperature dependence characteristic of hydrogen embrittlement. A discontinuous crack propagation, also characteristic of hydrogen embrittlement, was observed. Therefore, they concluded that the mechanism of stress-corrosion cracking in aluminum alloys involved hydrogen embrittlement.

EXPERIMENTAL OBJECTIVE

The objective of this investigation was to examine the hydrogen theory. If hydrogen ions have an effect on the fatigue life, then the fatigue life should be shorter as the hydrogen concentration in the aluminum is increased. In order to test this hypothesis, hydrogen was diffused into 2024-T351 aluminum specimens and fatigued in torsion. A comparison of the fatigue lives between the hydrogen-charged specimens and uncharged specimens should reveal if hydrogen does indeed affect the fatigue life of aluminum. Since Louthan and others (22) found that hydrogen charging had no effect on tensile properties of aluminum, it was decided to also include relative humidity as a variable in the experiment. Wilson (27) had shown in previous tests using the same fatigue testing equipment and the same type of aluminum alloy that a high humidity environment (85-90%) reduced the fatigue life of specimens up to 50% over the fatigue life of specimens in a low humidity environment (20-25%). With both hydrogen charging and humidity as variables, any interacting effect can be considered.

TEST APPARATUS

The test apparatus can be broken down into two major catagories: diffusion equipment and fatigue equipment.

Diffusion Equipment

The diffusion equipment consisted of two high-pressure autoclaves, two pressure gages, an autoclave heater, and a temperature-control device. Figure 1 shows this equipment. The autoclaves and pressure gages provided the means of keeping the specimens in a high-pressure hydrogen environment for an extended period of time so that hydrogen could diffuse into them. The heater was used to raise the temperature of the specimens in order to increase their diffusitivity.

Fatigue Equipment

The fatigue equipment consisted of a fatigue machine, an environmental chamber, a humidifying unit, an air supply, and an electric hygrometer.

The fatigue machine was a Sonntag Universal Fatigue Testing Machine (Figs. 2 and 3). The motor operated at 1800 rpm and produced a vertical-vibratory force of constant amplitude by rotation of an unbalanced mass. This force acted through a torisonal fixture (Fig. 4) to produce completely reversed torsion in the specimen. The amount of torsion was controlled by adjusting the eccentricity of the unbalanced rotating mass. A reset counter indicated thousands of stress cycles to failure. One of two limit switches stopped the machine when the amplitude of the vibration increased due to failure of the specimen.

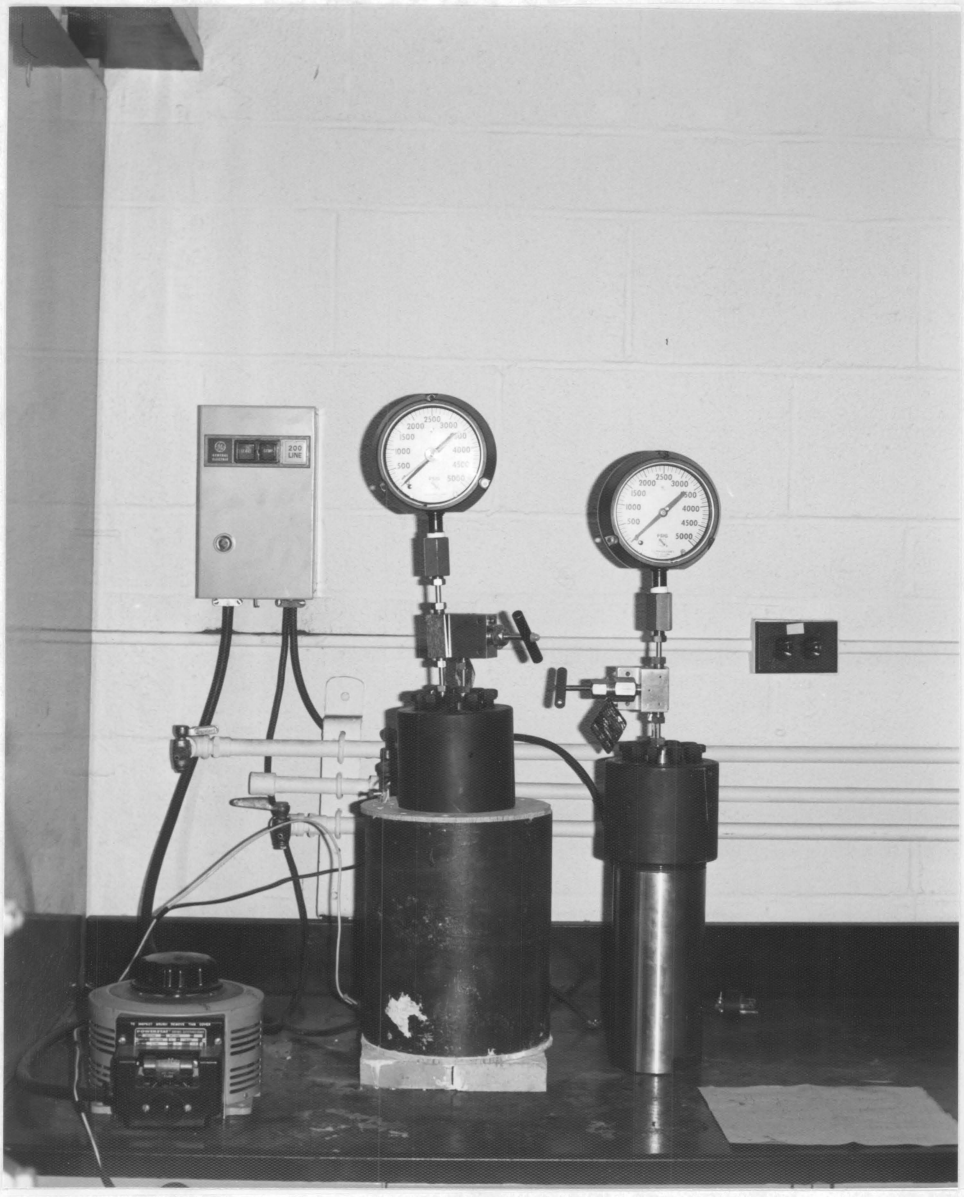

FIGURE 1. DIFFUSION EQUIPMENT

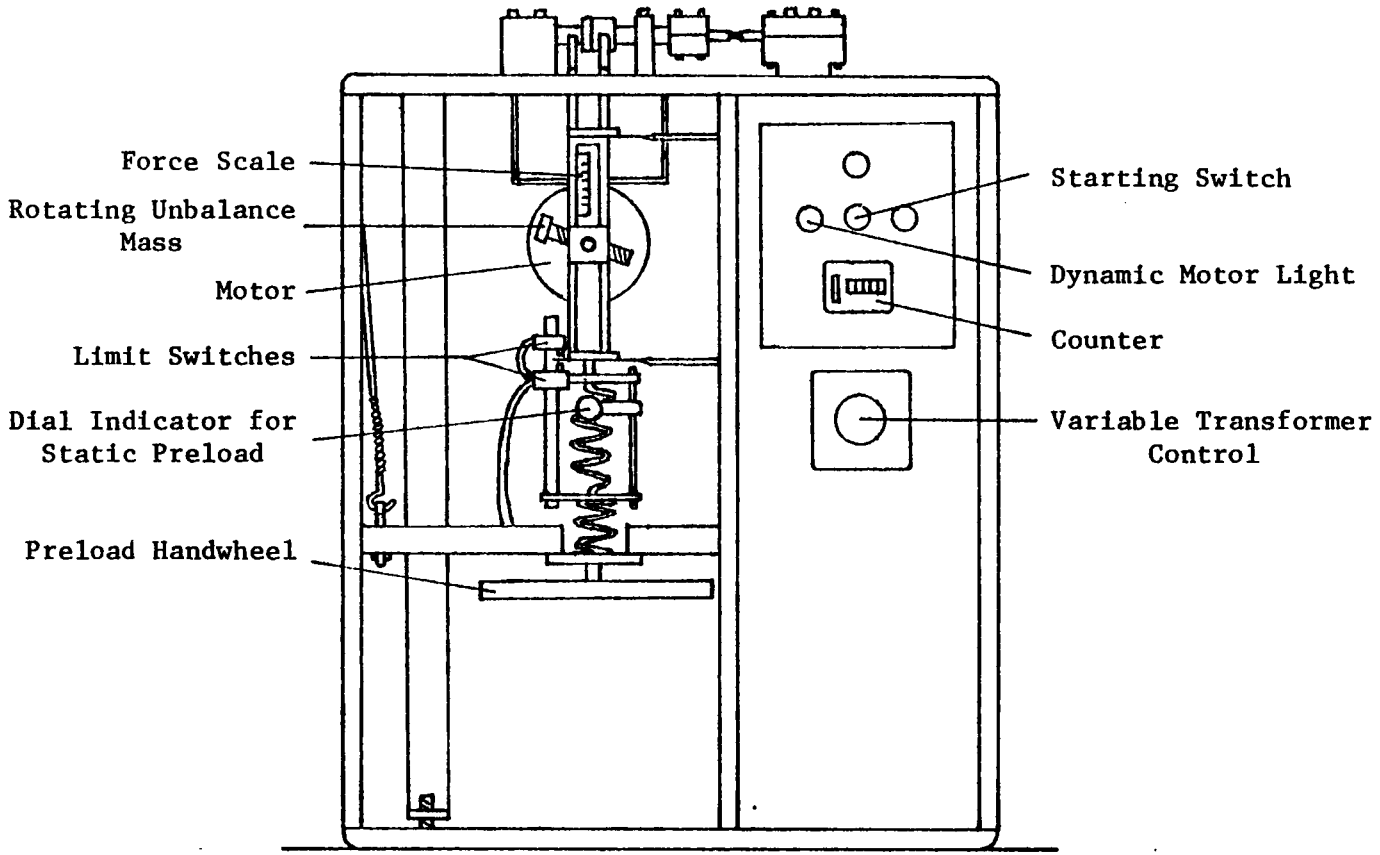

FIGURE 2. SCHEMATIC DRAWING OF SONNTAG UNIVERSAL FATIGUE TESTING MACHINE COMPONENTS [From Womack (28)]

FIGURE 3. SONNTAG UNIVERSAL FATIGUE TESTING MACHINE WITH ENVIRONMENTAL CHAMBER IN PLACE

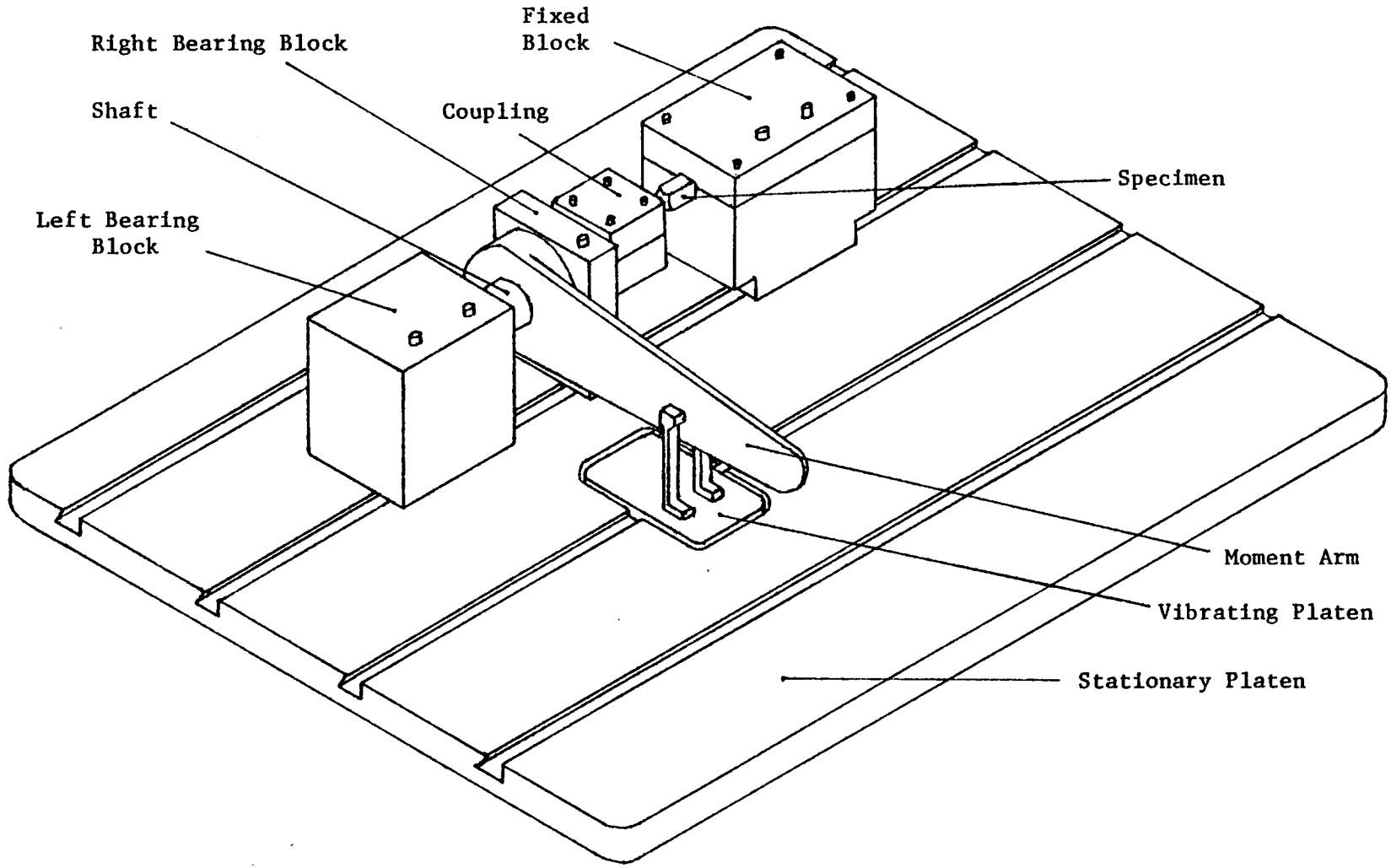

FIGURE 4. SCHEMATIC DRAWING OF TORSIONAL FIXTURE COMPONENTS
From Womack (28)

The environmental chamber consisted of a plastic sleeve around the test specimen attached to the fixed block and the coupling by wide rubber bands, as shown in Figure 5. The controlled air entered through a tube on one side of the environmental chamber creating a positive pressure. This insured that the proper humidity was maintained in the chamber.

The humidifying unit (Fig. 6) contains a heater, a chiller, a centrifugal pump, and a bubble tower. The centrifugal pump continually circulates a water and ethylene-glycol solution through the other components of the system. In the bubble tower, air was bubbled through distilled water to obtain the humidity level desired. High humidity (85 - 90%) required that the distilled water be heated. Low humidity (20 - 25%) required cooling of the distilled water. A thermostat on the bubble tower regulated the temperature of the water, keeping the humidity of the air within the required limits which are stated above.

The air was taken from the laboratory air supply. After passing through a regulator and a filter, the air entered the bubble tower of the humidifying unit. From the bubble tower, the now humid air passed through two condensation jars and a coil of plastic tubing. This permitted the air to return to the room temperature of 72° - 74°F [22° - 23°C]. Then the air passed through a flow meter, a final condensation jar, a plexiglas instrumentation chamber, and finally through a tube into the environmental chamber. The air flow rate into the chamber was approximately 1.0 cfm [$4.7 \times 10^{-4} m^3/s$].

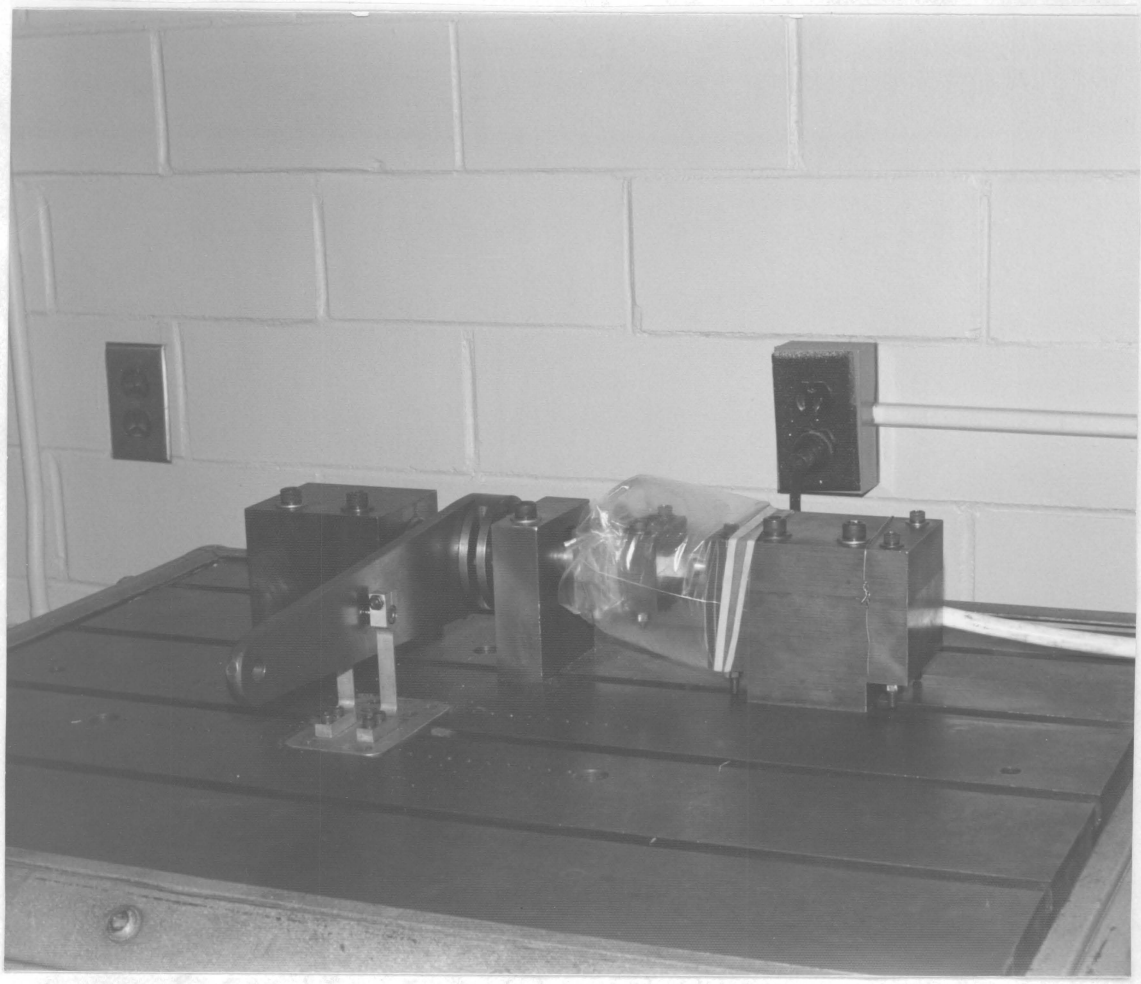

FIGURE 5. TORSIONAL FIXTURE OF FATIGUE TESTING MACHINE WITH ENVIRONMENTAL CHAMBER IN PLACE

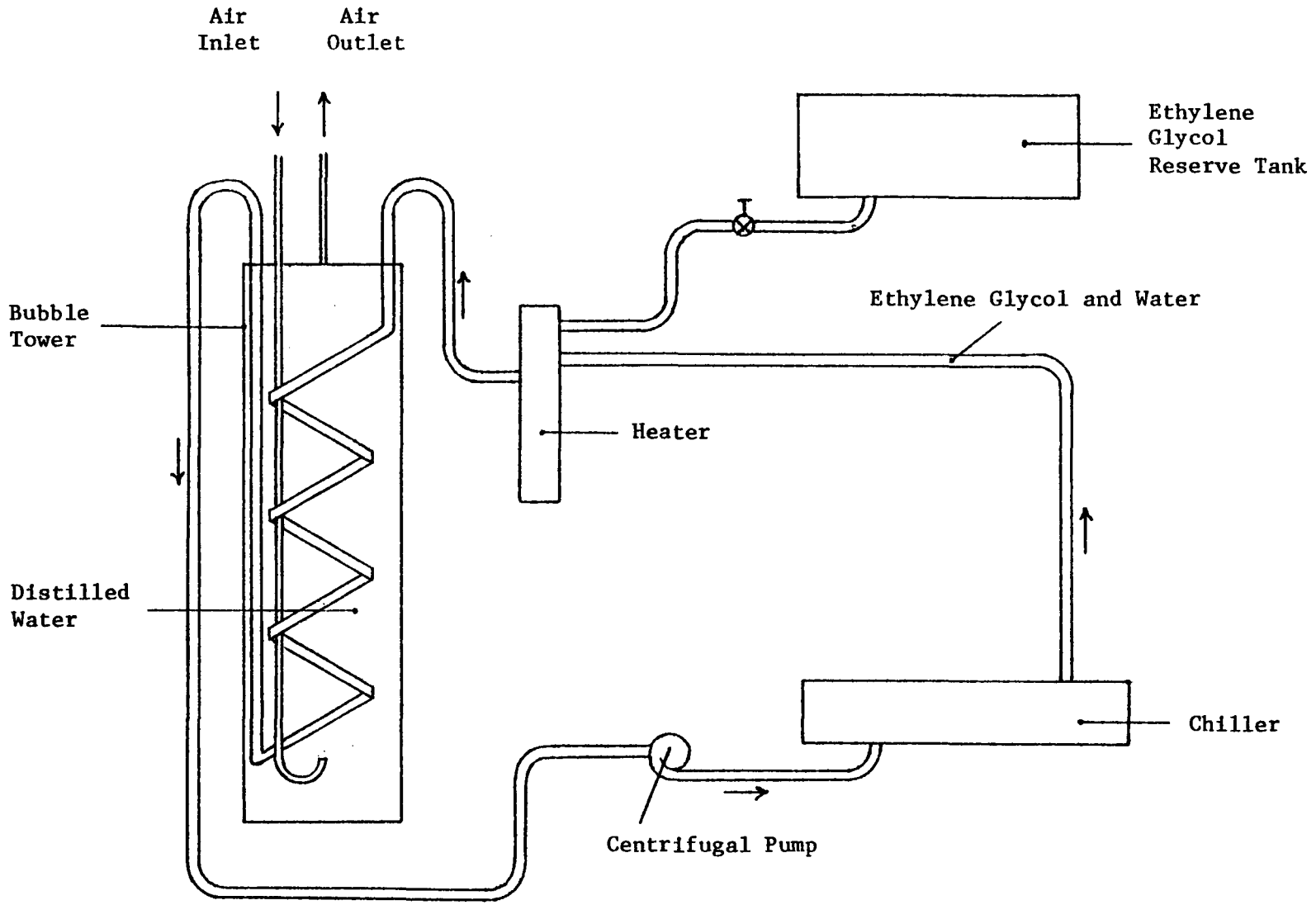

FIGURE 6. SCHEMATIC DRAWING OF HUMIDIFYING EQUIPMENT

The instrumentation chamber housed a thermometer and an electric hygrometer sensor. This gave a continual reading of the dry bulb temperature and the relative humidity of the air entering the environmental chamber.

TEST SPECIMENS

The test specimens were made from extruded ½-inch [12.7 mm] square bar stock of 2024-T351 aluminum. Mechanical properties, mechanical property limits, and chemical composition of this aluminum alloy are given in Tables 1, 2, and 3, respectively. The specimens were cut in 4 in. [102 mm] lengths and machined to a minimum diameter of 0.362 $\pm$ 0.0015 in. [9.195 $\pm$ 0.0381 mm] in the center as shown in Figure 7. Each test specimen was numbered in sequence after machining.

TABLE 1

MECHANICAL PROPERTIES OF 2024-T351 ALUMINUM

	Typical*	Tests-Minimum**
Ultimate Tensile Strength	68 ksi [470 MPa]	62 ksi [430 MPa]
Tensile Yield Strength	47 ksi [320 MPa]	45 ksi [310 MPa]
Percent Elongation in 2 in. (50.8 mm)	19	10
Brinell Hardness	120	
Ultimate Shear Strength	41 ksi [280 MPa]	
Modulus of Elasticity	10.6×10^3 ksi [73100 MPa]	

*Aluminum Standards and Data, Second Edition, The Aluminum Association, New York, N.Y., 1969, p. 27. (Ref. 29)

**"Certificate of Aluminum Analysis", Williams and Company, Inc., Pittsburgh, Pa., Order No. B 747862 7 03, November 29, 1977. (Ref. 30)

TABLE 2

MECHANICAL PROPERTY LIMITS OF EXTRUDED SHAPES

OF 2024-T351 ALUMINUM*

For Diameter or Thickness of 0.250 - 0.749 in. [6.35 - 19.0 mm]

Ultimate Tensile Strength (min.)	60.0 ksi [410 MPa]
Tensile Yield Strength (min.)	44.0 ksi [300 MPa]
Percent Elongation in 2 in [50.8 mm] (min.)	12

*Aluminum Standards and Data, Second Edition, The Aluminum Association, New York, N.Y., 1969, p. 135. (Ref. 29)

TABLE 3

CHEMICAL COMPOSITION OF 2024 ALUMINUM*

(In weight percent)

Zinc	0.25 Max.
Magnesium	1.2 - 1.8
Copper	3.8 - 4.9
Iron	0.50 Max.
Silicon	0.50
Manganese	0.30 - 0.90
Chromium	0.10
Others	0.15 (Each not exceeding 0.05)

*Speidel, M. O., and Hyatt, M. V., "Stress-Corrosion Cracking of High-Strength Aluminum Alloys," Advances in Corrosion Science and Technology, Vol. 2, Plenum Press, 1972, p. 116. (Ref. 31)

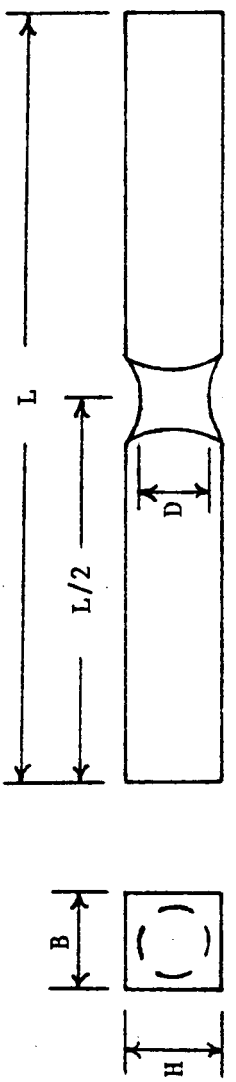

	in.	mm
L	4.00	102
D	0.362	9.19
B	0.50	12.7
H	0.50	12.7

FIGURE 7. TEST SPECIMEN DIMENSIONS

TEST PROCEDURE

In order to prevent any variability in the original bar stock or any machining effects from biasing the fatigue life results, all of the test specimens were randomized according to the results of a random number generator. However, it was not practical to randomize the two levels of relative humidity or the three levels of stress. The specimens were then divided into two groups, one to undergo hydrogen charging and the other to remain as a control group. Both groups were soaked for 12 hours in methyl alcohol at room temperature and then wiped with a soft cotton cloth to remove any oil film or dirt that may have collected on the machined surface.

The group to be charged with hydrogen was subdivided into two subgroups and placed in two separate high-pressure autoclaves. Both autoclaves were evacuated and then pressurized with hydrogen (>99.5% pure) to 1500 psi [10 MPa] at room temperature. One autoclave was then placed in the autoclave heater where the temperature was raised to approximately 121°C [250°F] at a pressure of approximately 2000 psi [14 MPa]. The other autoclave was left at room temperature. After 25 days under these conditions, the first autoclave was removed from the heater and the second autoclave placed in the heater. The second autoclave was maintained at the same temperature and pressure as the first autoclave for 25 days. The specimens were taken out of the autoclaves as soon as possible after removal of the autoclave from the heater and then stored in a freezer at 25°F [-4.4°C] until tested. This was done to delay the hydrogen from diffusing out of the specimens.

The control group was placed in an oven at 250°F [121°C] for 25 days, also. This was done to eliminate any temperature effects between the hydrogen charged and the uncharged specimens. After removal from the oven, the uncharged samples were kept in a "clean room" at room temperature.

Charged specimens were run in groups of six at each of three different stress levels at high humidity (85 - 90%). These completely reversed stress levels were approximately 13,400, 16,800, and 20,100 psi [89.6, 117, and 138 MPa]. Then uncharged specimens were run in groups of six at each of the three stress levels at high humidity. Low humidity (20 - 25%) tests for charged and uncharged specimens were conducted in the same manner.

The stresses are shear stresses calculated from the shear stress formula for round objects shown below where all dimensions are based on the reduced section.

$$\tau = \frac{Tr}{J}$$

where:

τ = shear stress, psi [Pa].

T = torque on specimen (moment arm length times the force produced by the unbalanced mass on the fatigue machine) lbs - in. [N · m].

r = radius, in. [m].

J = polar moment of inertia of the cross section, $in.^4$ [m^4].

The rectangular surfaces of all specimens were hand sanded slightly before testing so that they would fit into the fixed block and the coupling block. The machined test sections were not sanded. Only charged specimens from the first autoclave were used in the high humidity tests and only charged specimens from the second autoclave were used in the low humidity tests.

RESULTS

The results of this investigation are displayed in Table 4. Fatigue life data have been found to approach a straight line when the number of cycles is plotted in logarithmic form against stress. Therefore, semi-logarithmic curves were fitted by the method of least squares to the data for each humidity level and charging condition. These curves are the S-N diagrams shown in Figs. 8, 9, 11, and 12. A comparison between charged and uncharged specimens at high relative humidity is shown in Fig. 10. The same comparison at low relative humidity is given in Fig. 13. The numbers next to data points on these figures indicate the number of data points at that location.

A difference in the type of cracks observed between charged and uncharged specimens at the high relative humidity is shown in Table 4. The cracks in charged specimens were predominately diagonal cracks at 45° to the horizontal, characteristic of brittle fractures under torsional loads. The cracks in the uncharged specimens were predominately circumferential cracks characteristic of failures in ductile materials. A typical 45° crack with some branching is shown in Fig. 14a. A circumferential crack is shown in Fig. 14b. This distinct difference in crack propagation angle was not evident at the low relative humidity.

Examination of the fracture surfaces with a scanning electron microscope produced a mixture of results. Figures 15 and 16 show the fracture surfaces of two hydrogen-charged specimens fatigued under high humidity at 20,100 psi [138 MPa] and 16,800 psi [117 MPa]

respectively. Both specimens underwent diagonal cracking. The striations visible in Fig. 15 are typical of those that occur with hydrogen embrittlement. However, Fig. 16 shows no such striation pattern even though the only difference in the two specimens is the stress level. Figure 17 shows the fracture surface of an uncharged specimen that cracked circumferentially while running at 20,100 psi [138 MPa] under high humidity. As expected, there are no striations in the uncharged specimen shown in Fig. 17.

TABLE 4

RESULTS FOR FATIGUE TESTS

STRESS	HUMIDITY	CONDITION	CYCLES	CRACK TYPE*
20,100 psi [138 MPa]	HIGH	CHARGED	406,000	D
			727,000	D
			598,000	D&C
			724,000	D
			383,000	D
			465,000	C
16,800 psi [117 MPa]	HIGH	CHARGED	740,000	D
			804,000	D
			3,615,000	D
			1,762,000	D
			425,000	D
			3,552,000	D&C
13,400 psi [89.6 MPa]	HIGH	CHARGED	10,305,000**	---
			8,279,000**	---
			10,271,000**	---
			1,034,000	D
			8,105,000**	---
			1,095,000	D

*D - Diagonal, C - Circumferential.
**No Failure

TABLE 4 (Cont'd)

RESULTS FOR FATIGUE TESTS

STRESS	HUMIDITY	CONDITION	CYCLES	CRACK TYPE*
20,100 psi [138 MPa]	HIGH	UNCHARGED	236,000	C
			106,000	C
			293,000	C
			433,000	C
			791,000	C
			310,000	C
16,800 psi [117 MPa]	HIGH	UNCHARGED	497,000	C
			1,119,000	C
			2,125,000	C
			959,000	C
			2,441,000	C
			1,637,000	C
13,400 psi [89.6 MPa]	HIGH	UNCHARGED	4,816,000	C
			3,029,000	C
			1,203,000	C
			1,101,000	C
			821,000	C
			1,015,000	D

*D - Diagonal, C - Circumferential.

TABLE 4 (Cont'd)

RESULTS FOR FATIGUE TESTS

STRESS	HUMIDITY	CONDITION	CYCLES	CRACK TYPE*
20,100 psi [138 MPa]	LOW	CHARGED	2,052,000	C
			503,000	C
			1,108,000	C
			2,242,000	C
			3,551,000	C
			2,488,000	C
16,800 psi [117 MPa]	LOW	CHARGED	1,537,000	C
			6,061,000	D&C
			6,537,000	D&C
			3,541,000	D
			4,293,000	D&C
			5,261,000	D&C
13,400 psi [89.6 MPa]	LOW	CHARGED	8,248,000**	---
			7,419,000	D
			8,122,000**	---
			8,012,000**	---
			8,195,000**	---
			8,019,000**	---

*D - Diagonal, C - Circumferential.
**No Failure

TABLE 4 (Cont'd)

RESULTS FOR FATIGUE TESTS

STRESS	HUMIDITY	CONDITION	CYCLES	CRACK TYPE*
20,100 psi [138 MPa]	LOW	UNCHARGED	5,104,000	C
			2,274,000	C
			5,570,000	C
			982,000	C
			2,104,000	C
			1,428,000	C
16,800 psi [117 MPa]	LOW	UNCHARGED	3,148,000	D&C
			4,906,000	D&C
			9,867,000**	---
			5,974,000	D&C
			4,879,000	C
			8,877,000**	---
13,400 psi [89.6 MPa]	LOW	UNCHARGED	8,024,000**	---
			8,018,000**	---
			8,141,000**	---
			8,416,000**	---
			5,638,000	D&C
			8,492,000**	---

*D - Diagonal, C - Circumferential.
**No Failure

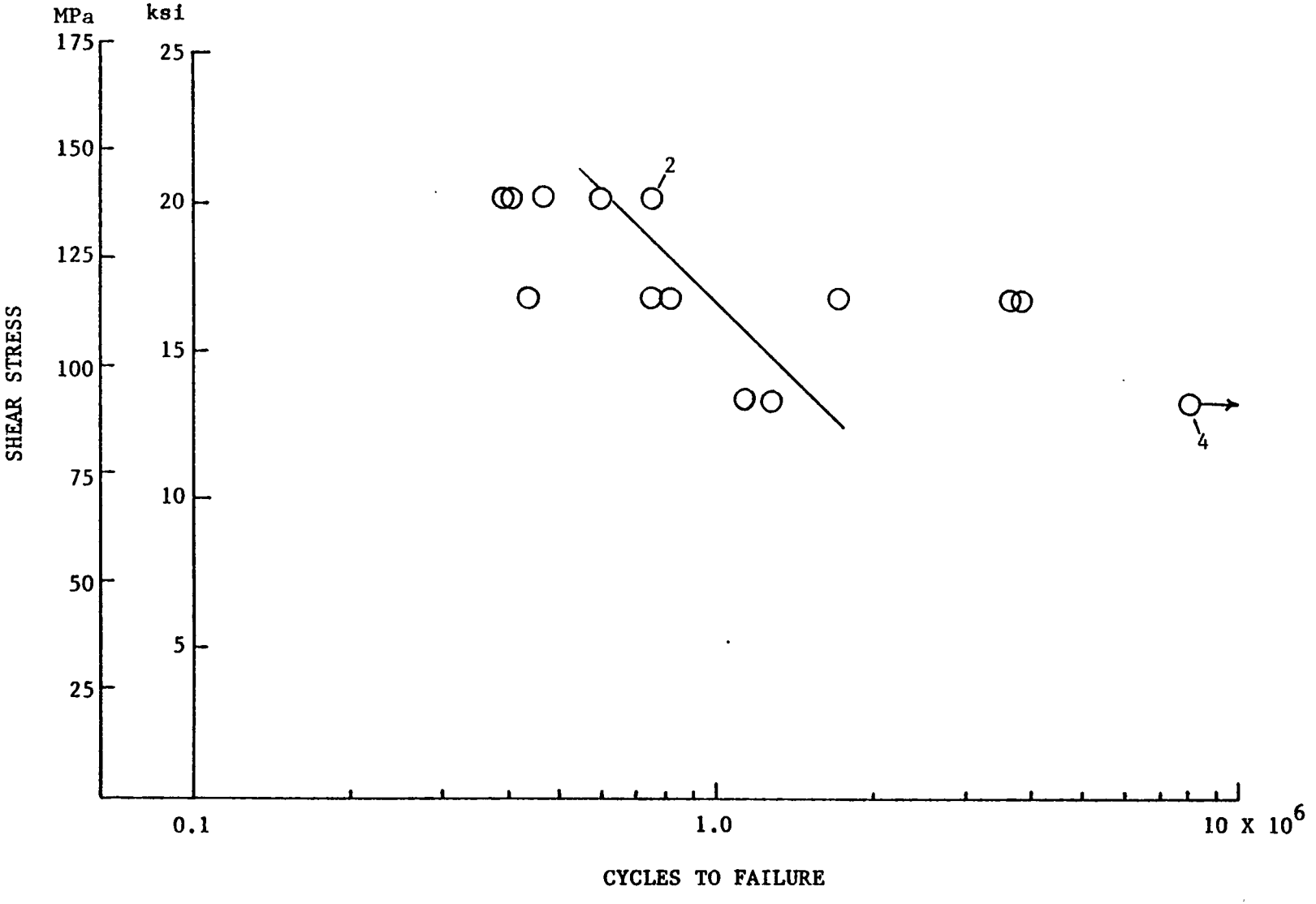

FIGURE 8. TESTS AT HIGH RELATIVE HUMIDITY FOR CHARGED SPECIMENS

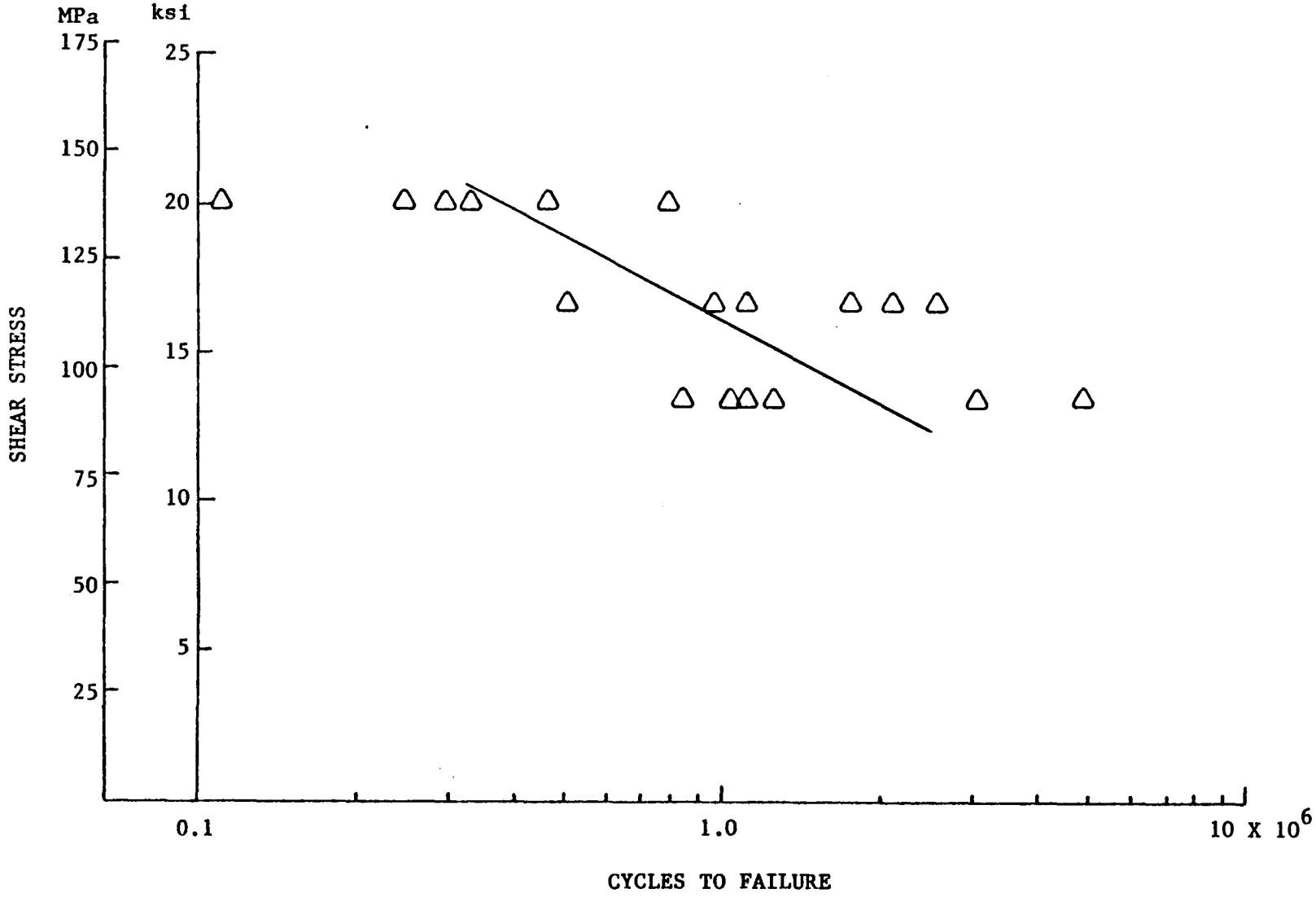

FIGURE 9. TESTS AT HIGH RELATIVE HUMIDITY FOR UNCHARGED SPECIMENS

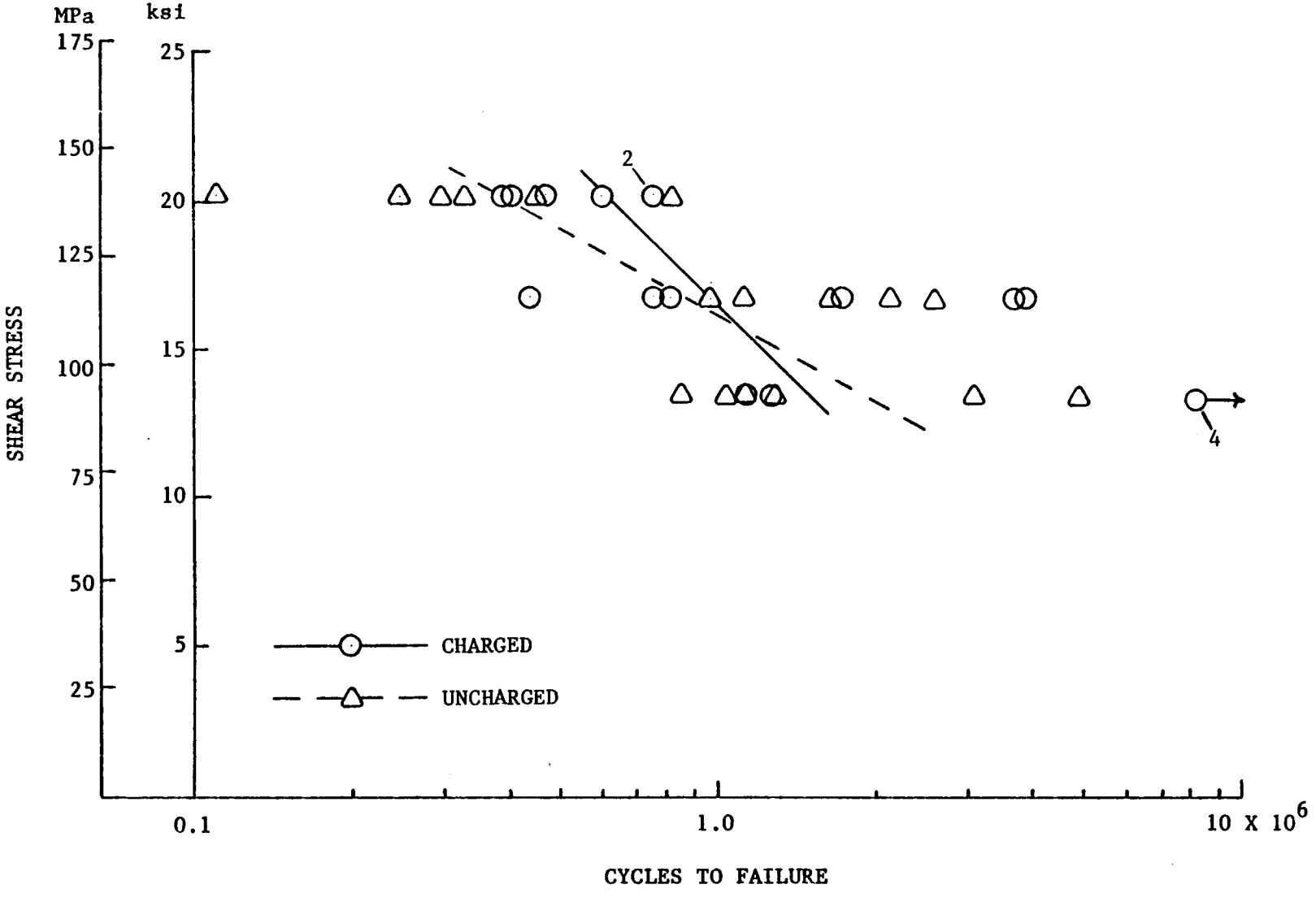

FIGURE 10. COMPARISON OF TESTS AT HIGH RELATIVE HUMIDITY FOR CHARGED AND UNCHARGED SPECIMENS

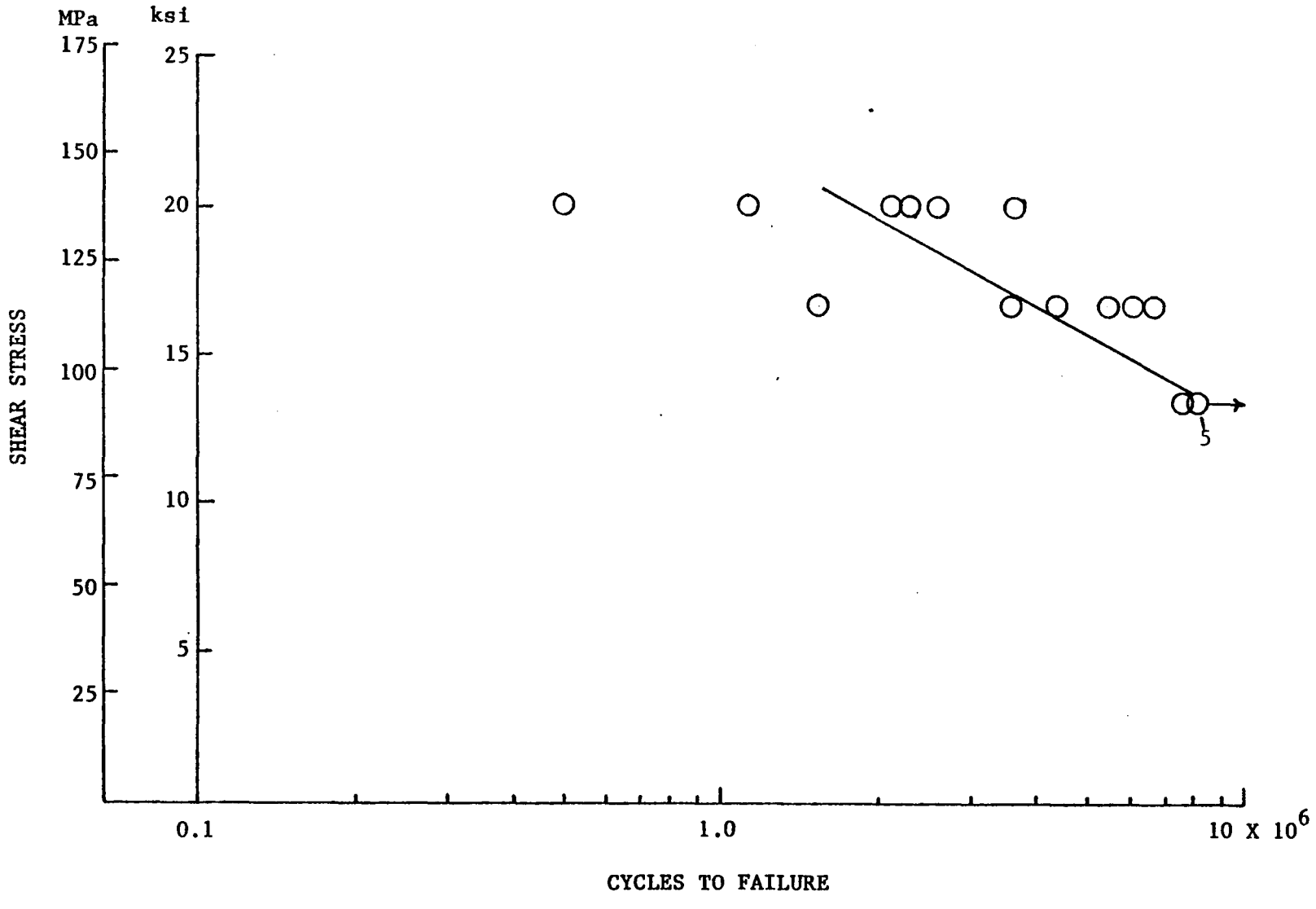

FIGURE 11. TESTS AT LOW RELATIVE HUMIDITY FOR CHARGED SPECIMENS

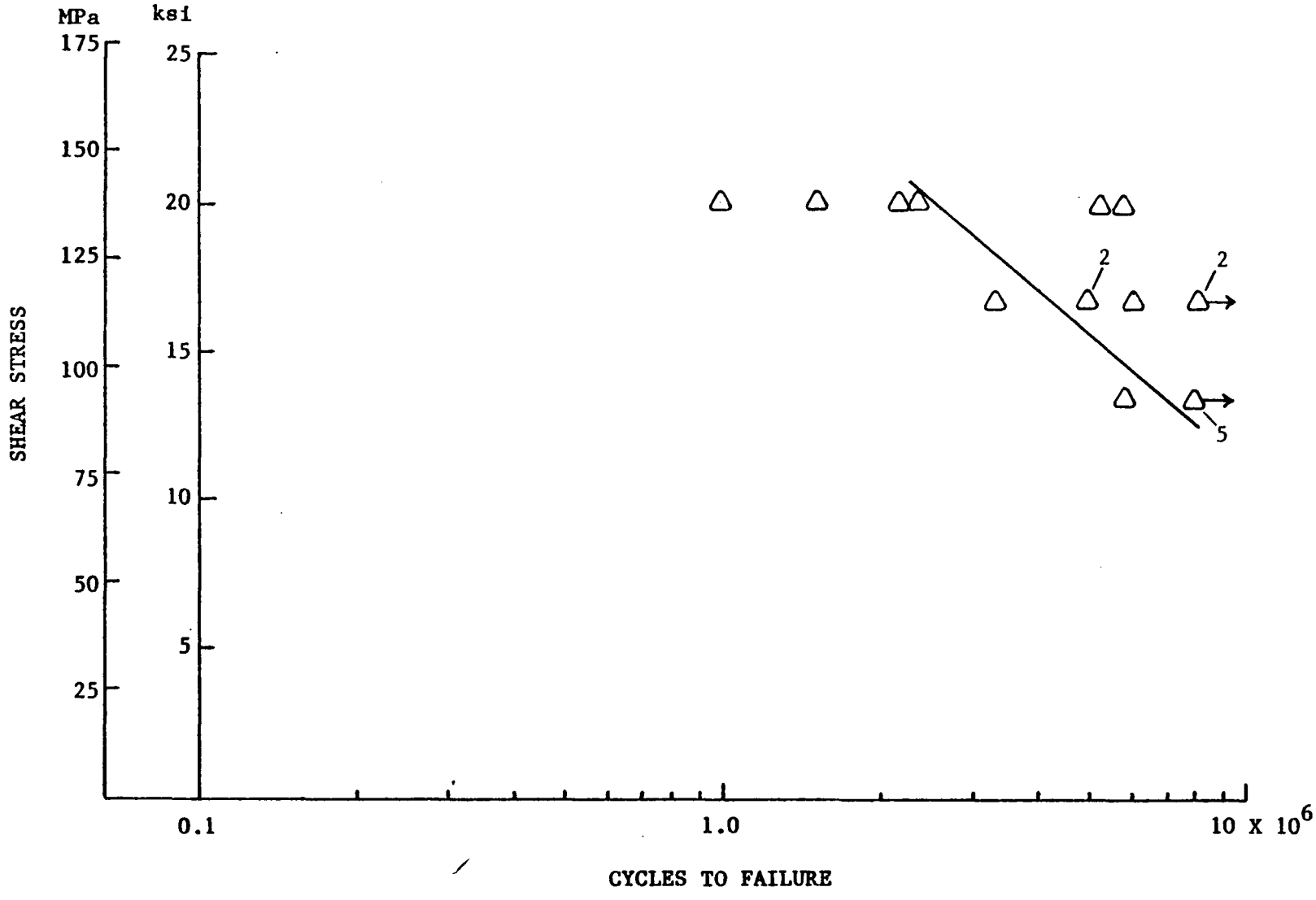

FIGURE 12. TESTS AT LOW RELATIVE HUMIDITY FOR UNCHARGED SPECIMENS

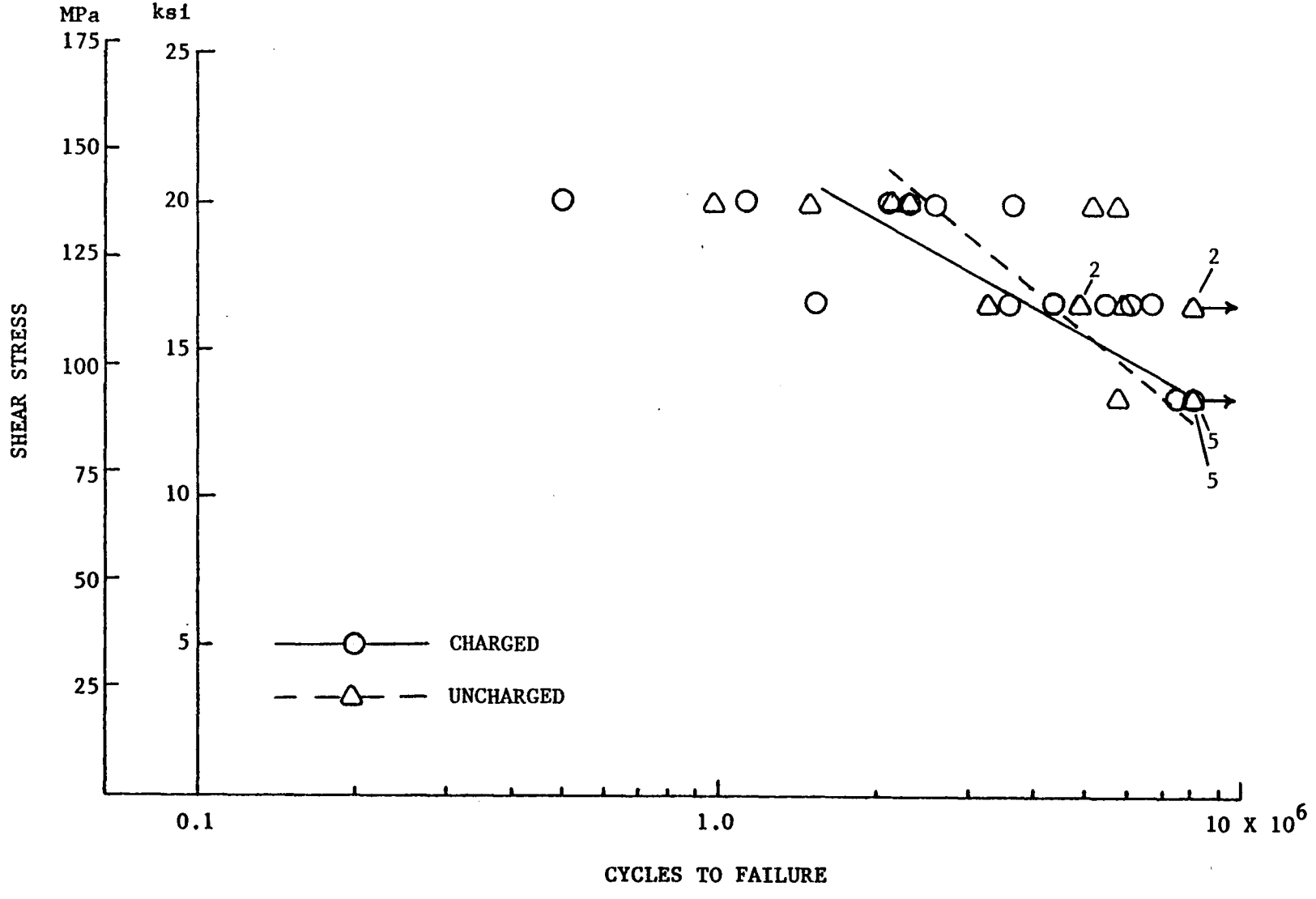

FIGURE 13. COMPARISON OF TESTS AT LOW RELATIVE HUMIDITY FOR CHARGED AND UNCHARGED SPECIMENS

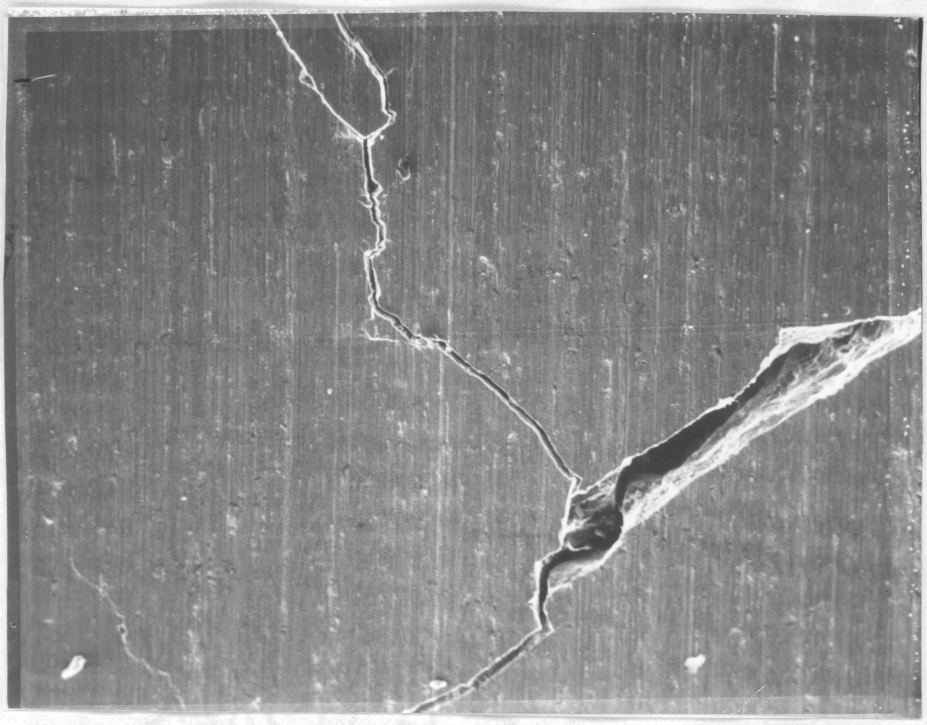

FIGURE 14a. TYPICAL CRACK PROPAGATION IN A HYDROGEN-CHARGED SPECIMEN AT HIGH HUMIDITY. 90X

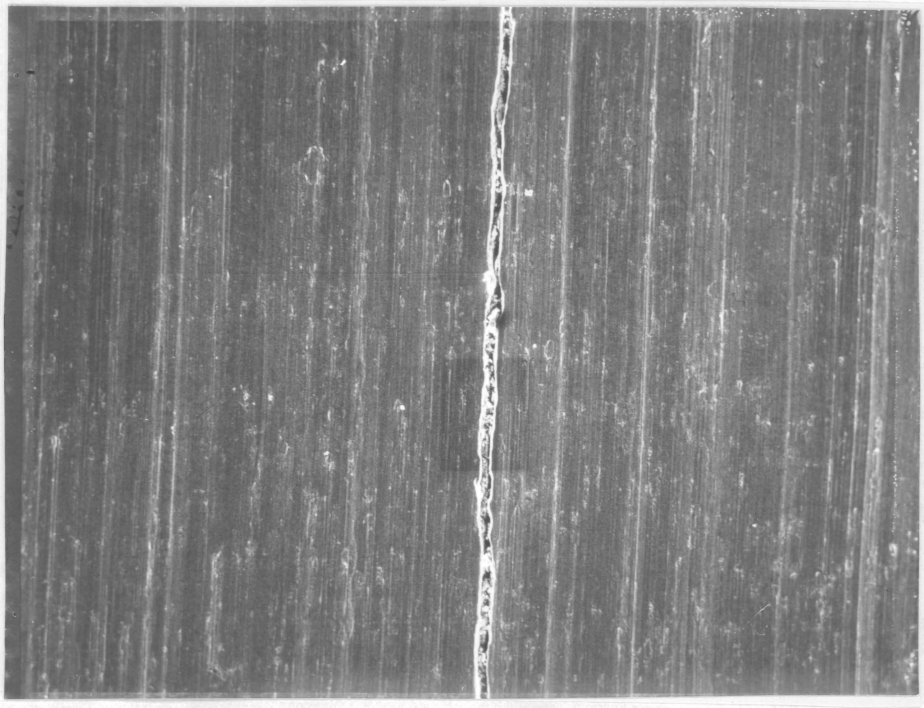

FIGURE 14b. TYPICAL CRACK PROPAGATION IN UNCHARGED SPECIMENS AND LOW HUMIDITY CHARGED SPECIMENS. 90X

FIGURE 15. FRACTURE SURFACE OF A HYDROGEN-CHARGED SPECIMEN SHOWING STRIATIONS. 180X
(High humidity, 20,100 psi 138 MPa stress)

FIGURE 16. FRACTURE SURFACE OF A HYDROGEN-CHARGED SPECIMEN SHOWING NO STRIATIONS. 180X
(High humidity 16,800 psi 117 MPa stress)

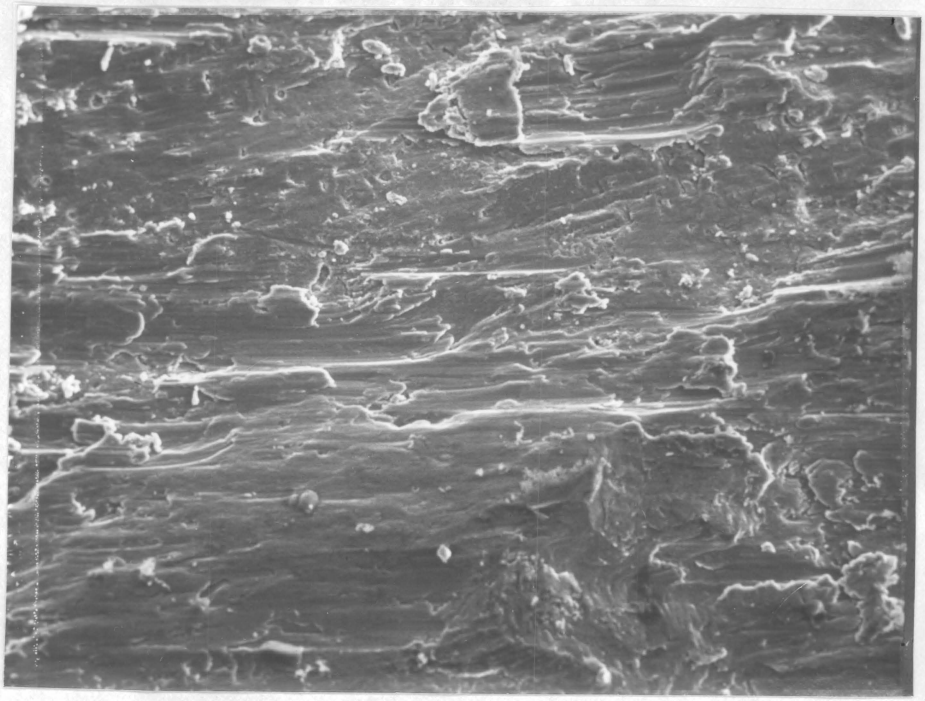

FIGURE 17. FRACTURE SURFACE OF AN UNCHARGED SPECIMEN SHOWING NO STRIATIONS. 200X
(High humidity 20,100 psi 138 MPa stress)

DISCUSSION OF RESULTS

The theory proposed by Broom and Nicholson (3) and supported by Hartman (7), Bradshaw and Wheeler (9), and Wei (15) suggested that hydrogen ions assisted crack initiation and growth in one of three ways:

1. Hydrogen diffuses into voids leading to a buildup of internal pressure.
2. Hydrogen associates with vacancies which enhance the chances of the vacancies clustering to form voids.
3. Hydrogen embrittles the aluminum by lowering the surface energy.

Of these three mechanisms, the hydrogen-embrittlement mechanism is supported by the change in crack propagation at high humidity from the ductile-type circumferential crack with uncharged specimens to the brittle-type diagonal crack with charged specimens. The observed striations typical of hydrogen embrittlement also support this mechanism.

Tests of significance were performed for the charged and uncharged specimens at both humidity levels. A F-ratio test of the variances and a t-test for the means indicate no significant differences at a 95% confidence level between charged and uncharged specimens at either high or low relative humidities. These results are displayed in Table 5. This indicates that the curves in Fig. 10 and Fig. 13 cannot be considered significantly different.

TABLE 5

RESULTS OF SIGNIFICANCE TESTS

	High Humidity		Low Humidity	
	Charged	Uncharged	Charged	Uncharged
Mean	5.9406	5.9308	6.4549	6.5168
Standard Deviation	0.3184	0.4239	0.3382	0.2722
Computed F	0.56		1.54	
Table F	2.36		2.91	
Computed t	0.072		0.487	
Table t	1.70		1.72	

The results above suggest either that diffused hydrogen has no effect on the fatigue life of aluminum or that insufficient hydrogen diffused through the oxide film into the aluminum. The latter possibility was the conclusion reached by McLellan and Harkins (24) from their studies. However, the change in crack propagation angle in this experiment at high hymidity suggests that some hydrogen was diffused into the aluminum specimens and that the specimens were embrittled to some extent. The significance of this change in type of crack is strengthened by the previous tests of Wilson (27) and Womack (28) on coated and uncoated aluminum specimens of the same type which displayed predominately circumferential cracks.

CONCLUSIONS

- No significant difference in fatigue life occurred between hydrogen charged specimens and uncharged specimens at high or low relative humidity.

- The change in crack propagation angle at high relative humidity from circumferential on uncharged specimens to diagonal on hydrogen charged specimens may be the result of hydrogen embrittlement.

RECOMMENDATIONS

Further investigation of the change in crack propagation angle should be undertaken. This might include:

Artifically aging specimens at high temperatures to embrittle them and then fatigue testing them to see if diagonal cracking occurs.

Torsional tensile testing of hydrogen charged and uncharged specimens to determine if any changes in properties occur.

Fatigue testing of additional specimens charged at higher pressures and temperatures to verify the results. (Specimens are now being charged at 3000 psi [21 MPa] and 250°C for this purpose.)

REFERENCES

1. Wadsworth, N. J., "The Effect of Environment on Metal Fatigue," Internal Stresses and Fatigue in Metals, Proceedings of the Symposium on Internal Stresses and Fatigue in Metals, 1958, Elsevier Publishing Co., 1959, pp. 382-396.

2. Wadsworth, N. J., and Hutchings, J., "The Effect of Atmospheric Corrosion on Metal Fatigue," Philosophical Magazine, Vol. 3, 1958, pp. 1154-1165.

3. Broom, T., and Nicholson, A., "Atmospheric Corrosion-Fatigue of Age-Hardened Aluminum Alloys," J. Inst. Metals, Vol. 89, February, 1961, pp. 183-190.

4. Holshouser, W. L., and Bennett, J. A., "Gas Evolution from Metal Surfaces During Fatigue Stressing," Proceedings ASTM, Vol. 62, 1962, pp. 683-693.

5. Laird, C., and Smith, G. C., "Initial Stages of Damage in High Stress Fatigue in Some Pure Metals," Philosophical Magazine, Vol. 8, 1963, pp. 1945-1962.

6. Bennett, J. A., "Effect of Reactions with the Atmosphere During Fatigue of Metals," Sagamore Army Materials Conference, 10th Fatigue--An Interdisciplinary Approach-Proceedings, August, 1963, pp. 209-227.

7. Hartman, A., "On the Effect of Oxygen and Water Vapor on the Propagation of Fatigue Cracks in 2024-T3 Alclad Sheet," Int. J. Fracture Mechanics, Vol. 1, September, 1965, pp. 167-188.

8. Hordon, M. J., "Fatigue Behavior of Aluminum in Vacuum," Acta Metallurgica, Vol. 14, 1966, pp. 1173-1178.

9. Bradshaw, F. J., and Wheeler, C., "The Effect of Environment on Fatigue Crack Growth in Aluminium and Some Aluminium Alloys," Applied Materials Research, Vol. 5, April, 1966, pp. 112-120.

10. Eeles, E. G., and Thurston, R. C. A., "The Relation of Humidity to the Fatigue Endurance of an Aluminium Alloy," J. Inst. Metals, Vol. 95, April, 1967, pp. 111-115.

11. Grosskreutz, J. C., "The Effect of Oxide Films on Dislocation-Surface Interactions in Aluminum," Surface Science, Vol. 8, 1967, pp. 173-190.

12. Meyn, D. A., "Observations on Micromechanisms of Fatigue Crack Propagation in 2024 Aluminum," ASM Trans. Quart., Vol. 61, March, 1968, pp. 42-50.

13. Meyn, D. A., "Nature of Fatigue-Crack Propagation in Air and Vacuum for 2024 Aluminum," ASM Trans. Quart., Vol. 61, March, 1968, pp. 52-61.

14. Wright, M. A., and Hordon, M. J., "Effect of Residual Gas Composition on the Fatigue Behavior of Aluminum," Trans. of the Metallurgical Society of AIME, Vol. 242, April, 1968, pp. 713-714.

15. Wei, R. P. "Fatigue-Crack Propagation in a High-Strength Aluminum Alloy," Int. J. Fracture Mechanics, Vol. 4, June, 1968, pp. 159-167.

16. Engelmaier, W., "Fatigue Behavior and Crack Propagation in 2024-T3 Aluminum Alloy in Ultrahigh Vacuum and Air," Trans. of the Metallurgical Society of AIME, Vol. 242, August, 1968, pp. 1713-1718.

17. Achter, M. R., "The Adsorption Model for Environmental Effects in Fatigue Crack Propagation," Scripta Metallurgica, Vol. 2, 1968, pp. 525-528.

18. Wei, R. P., and Landes, J. D., "The Effect of D_2O on Fatigue-Crack Propagation in a High-Strength Aluminum Alloy," Int. J. Fracture Mechanics, Vol. 5, March, 1969, pp. 69-71.

19. Vennett, R. M., and Ansell, G. S., "A Study of Gaseous Hydrogen Damage in Certain FCC Metals," ASM Trans. Quart., Vol. 62, December, 1969, pp. 1007-1013.

20. McCarroll, B., and Anderson, J. R., "Interactions of Hydrogen Atoms and Molecules with Aluminum Films," Surface Science, Vol. 17, October, 1969, pp. 458-461.

21. George, G. C., "The Effect of Environmental Relative Humidity Upon the Ultrasonic Fatigue Endurance of an Age Hardening Aluminum Alloy," Proceedings of Conference, Corrosion Fatigue: Chemistry, Mechanics and Microstructure, University of Connecticut, 1971, National Association of Corrosion Engineers, pp. 459-467.

22. Louthan, M. R., Jr., Caskey, G. R., Jr., Donovan, J. A., and Rawl, D. E., Jr., "Hydrogen Embrittlement of Metals," Mater. Sci. Eng., Vol. 10, 1972, pp. 357-368.

23. Jewett, R. P., Walter, R. J., Chandler, W. T., and Frohmberg, R. P., Hydrogen Environment Embrittlement of Metals, NASA Contract Report, NASA Cr-2163, March, 1973.

24. McLellan, R. B., and Harkins, C. G., "Hydrogen Interactions with Metals," Matl. Sci. Eng., Vol. 18, 1975, pp. 5-35.

25. Speidel, M. O., "Hydrogen Embrittlement of Aluminum Alloys?," Hydrogen in Metals, Proceedings of an International Conference on the Effects of Hydrogen on Materials Properties and Selection and Structural Design, September, 1973, Champion, Pa., No. 2 in the American Society for Metals, Materials/Metalworking Technology Series, pp. 249-273.

26. Gest, R. J., and Troiano, A. R., "Stress Corrosion and Hydrogen Embrittlement in an Aluminum Alloy," Corrosion, Vol. 30, August, 1974, pp. 274-279.

27. Wilson, J. H., "Effect of Relative Humidity on Fatigue of 2024-T3 Aluminum in Reverse Torsion," Master's Thesis, Virginia Polytechnic Institute and State University, Blacksburg, Virginia, March, 1973.

28. Womack, E. F., "Effect of Relative Humidity on Fatigue of Anodized 2024-T351 Aluminum in Completely Reversed Torsion," Master's Thesis, Virginia Polytechnic Institute and State University, Blacksburg, Virginia, December, 1973.

29. Aluminum Standards and Data, Second Edition, The Aluminum Association, New York, N.Y., 1969, p. 27, 135.

30. "Certificate of Aluminum Analysis," Williams and Company, Inc. Pittsburgh, Pa., Order No. B 74-7862 7 03, November 29, 1977.

31. Speidel, M. O., and Hyatt, M. V., "Stress-Corrosion Cracking of High-Strength Aluminum Alloys," Advances in Corrosion Science and Technology, Vol. 2, Plenum Press, 1972, p. 116.

32. Walpole, R. E., and Myers, R. H., Probability and Statistics For Engineers and Scientists, Macmillan Company, New York, 1972, pp. 407-414.

33. A Tentative Guide for Fatigue Testing and the Statistical Analysis of Fatigue Data, ASTM Special Technical Publication No. 91-A, by Committee E-9 on Fatigue, American Society for Testing Materials, Philadelphia, Pa., 1967, p. 16.

APPENDIX A

STATISTICAL ANALYSIS OF RESULTS

The following steps were applied to the data in order to interpret the results.

1) A linear regression by the method of least squares was used to fit the data to a logarithmic curve of the form:

$$S = a + b \log(N)$$

where S = stress,

N = cycles to failure.

This plots as a straight line on semi-logarithmic paper and gives the familiar S-N diagram used in fatigue analysis. The equations for each condition are shown in Table A-1. The data for specimens that did not fail were not included in the analysis.

2) A correlation coefficient (R) was determined for each curve. This indicates how closely the equation for the curve fits the experimental data. The closer the value of R is to $\pm$ 1, the better the fit.

3) A F-statistic was used to determine if a significant difference in the standard deviations occurred between charged and uncharged specimens at each humidity level. The number of cycles to failure was converted to logarithmic form for these calculations since it has been

TABLE A - 1

EQUATIONS FOR S-N DIAGRAMS

HIGH HUMIDITY		
Charged	$S = 111629 - 15807 \log(N)$	$R = -0.482$
Uncharged	$S = 72220 - 9350 \log(N)$	$R = -0.710$
LOW HUMIDITY		
Charged	$S = 79075 - 9452 \log(N)$	$R = -0.677$
Uncharged	$S = 115835 - 14968 \log(N)$	$R = -0.562$

Note: S = Stress in psi.

N = Cycles to Failure.

found by others (33) that fatigue data approaches a normal distribution when this is done. The equation used was as follows:

$$F_{comp} = \frac{S_1^2}{S_2^2}$$

where S_1 = standard deviation of charged specimens

S_2 = standard deviation of uncharged specimens

If $\frac{1}{F_{table}} < F_{comp} < F_{table}$, then the standard deviations are considered to be not significantly different. At both humidities the standard deviations between charged and uncharged specimens were not significantly different at a 95% confidence level.

4) A t-statistic was used to determine if a significant difference in the means occurred between charged and uncharged specimens at both humidity levels. Since the standard deviations were not significantly different, a common variance was computed by the equation

$$S^2 = \frac{(n_1 - 1)\, S_1^2 + (n_2 - 1)\, S_2^2}{n_1 + n_2 - 2}$$

where S^2 = common variance

S_1 = standard deviation of charged specimens

S_2 = standard deviation of uncharged specimens

n_1 = number of charged specimens

n_2 = number of uncharged specimens

This common variance was then used to compute the t-statistic by the equation:

$$t_{comp} = \frac{\bar{X}_1 - \bar{X}_2}{S\sqrt{\frac{1}{n_1} + \frac{1}{n_2}}}$$

where $\bar{X}_1$ = mean of charged specimens

$\bar{X}_2$ = mean of uncharged specimens

The means for both humidities were found to be not significantly different at a 95% confidence level since t_{comp} was less than t_{table}. The computations for these statistics are given in Table A-2.

TABLE A-2

COMPUTATIONS FOR SIGNIFICANCE TESTS

High Humidity		Low Humidity	
Charged	Uncharged	Charged	Uncharged
5.6085	5.3729	6.3122	6.7079
5.8615	5.0253	5.7016	6.3568
5.7767	5.4669	6.0445	6.7459
5.8597	5.6365	6.3506	5.9921
5.5832	5.8982	6.5504	6.3230
5.6675	5.4914	6.3959	6.1547
5.8692	5.6964	6.1867	6.4980
5.9053	6.0488	6.7825	6.6907
6.5581	6.3274	6.8154	6.7763
6.2460	5.9818	6.5491	6.6883
5.6284	6.3876	6.6328	6.7511
6.5505	6.2140	6.7211	71.6848
6.0145	6.6827	6.8703	
6.0394	6.4813	83.9131	
83.1685	6.0813		
	6.0418		
	5.9143		
	6.0065		
	106.7551		
Sample Size(n)	14	18	13	11
Mean ($\bar{X}$)	5.9406	5.9308	6.4549	6.5168
Standard Deviation (S)	0.3184	0.4239	0.3382	0.2722

TABLE A-2 (continued)

COMPUTATIONS FOR SIGNIFICANCE TESTS

High Humidity Calculations

$$F = \frac{(0.3184)^2}{(0.4239)^2} = 0.5642$$

$$S^2 = \frac{13(0.3184)^2 + 17(0.4239)^2}{14 + 18 - 2}$$

$$= 0.1458$$

$$t = \frac{5.9406 - 5.9308}{[0.1458(1/14 + 1/18)]^{1/2}}$$

$$= 0.072$$

Low Humidity Calculations

$$F = \frac{(0.3382)^2}{(0.2722)^2} = 1.5437$$

$$S^2 = \frac{12(0.3382)^2 + 10(0.2722)^2}{13 + 11 - 2}$$

$$= 0.0961$$

$$t = \frac{6.4549 - 6.5168}{[0.0961(1/13 + 1/11)]^{1/2}}$$

$$= -0.487$$

APPENDIX B

TEST EQUIPMENT

Diffusion Equipment

1. HIGH PRESSURE AUTOCLAVE (Cat. No. 41-4150, Series B 5770, 8000 psi max.), Autoclave Engineers, Erie, Pa.
   Use: To keep specimens in hydrogen environment to allow for diffusion.

2. ASHCROFT DURAGUAGE (0-5000 psig), Dresser Industries, Stratford, Conn.
   Use: To indicate hydrogen pressure in the autoclave.

3. CHROMEL-ALUMEL THERMOCOUPLE TEMPERATURE CONTROLLER (Model No. 434-806R6).
   Use: To control the temperature of the autoclave.

4. POWERSTAT VARIABLE AUTOTRANSFORMER (Type 3PF236B), Superior Electric Co., Bristol, Conn.
   Use: To control the voltage going to the autoclave heater.

5. AUTOCLAVE HEATER, unknown heating element, built by N. Sridhar, VPI&SU.
   Use: To heat the autoclave.

6. TINNEY MITE 5 (Model T-5-20200), Tinney Engineering, Inc., Union, N.J.
   Use: To heat control specimens.

Fatigue Equipment

7. UNIVERSAL FATIGUE TESTING MACHINE (Model SF-01-U), Sonntag Scientific Corporation, Greenwich, Conn.
   Use: To apply reverse torsion to the specimen.

8. VAN-AIR FILTER (Model No. F5), Van Products Co., Erie, Pa.
   Use: To filter the laboratory air supply.

9. FISCHER AND PORTER FLOWMETER (Tube No. FP 1/4-20-G-5/81) Fischer and Porter Co., Hatboro, Pa.
   Use: To indicate the air flow into the environmental chamber.

10. ELECTRIC HYGROMETER INDICATOR (Cat. No. 4-5170), American Instrument Company, Inc., Silver Springs, Md.
    Use: To indicate the relative humidity of the air flow into the environmental chamber.

11. BELL AND GOSSET CENTRIFUGAL PUMP (Model No. 100 P 7-4), Bell and Gosset, Inc., Morton Grove, Ill.
    Use: To circulate the ethylene glycol and water mixture through the humidifying unit.

12. LEHIGH BLU-COLD COMMERCIAL REFRIGERATOR (Model AM42F FY 12), Lehigh Manufacturing Co., Lancaster, Pa.
    Use: To cool the ethylene glycol and water mixture for low humidities.

13. HEATING ELEMENT (Model No. D-230-U), Electro-Therm, Inc., Laurel, Md.
    Use: To heat the ethylene glycol and water mixture for high humidities.

Other Equipment

14. SCANNING ELECTRON MICROSCOPE (Model AMR-900), Advance Metals Research Corp., Burlington, Mass.
    Use: To microscopically examine fracture surfaces.

The vita has been removed from the scanned document

THE EFFECT OF DIFFUSED HYDROGEN ON THE TORSIONAL FATIGUE LIFE OF 2024-T351 ALUMINUM ALLOY

by

Charles Joseph Kauffmann, Jr.

(ABSTRACT)

Fatigue tests in reversed torsion were run on 2024-T351 aluminum alloy specimens into which hydrogen had been diffused. The diffusion was accomplished by placing the specimens in a hydrogen environment (>99.5%) for 25 days at 2000 psi [13.8 MPa] and 123°C. A control group was tested which underwent the same temperature conditions for 25 days. The fatigue tests were run at low (20-25%) and high (85-90%) relative humidities and at shear stress levels of approximately 13400, 16800, and 20100 psi [89.6, 117, and 138 MPa].

The results of this investigation show that hydrogen charging has no effect on the torsional fatigue life of aluminum. However, a change in the crack propagation angle at high relative humidity for a ductile, circumferential crack on uncharged specimens to a brittle, 45° crack on hydrogen-charged specimens may be the result of hydrogen embrittlement.